Alteration of Major Cellular Organelles in Wheat Leaf Tissue Infected with Wheat Streak Mosaic Rymovirus (Potyviridae)

Jian-Guo Gao and Annette Nassuth

Department of Botany, University of Guelph, Guelph, Ontario, Canada N1G 2W1.

We thank J. S. Greenwood for comments on the manuscript and A. Moore for technical advice. The assistance of W. Matthes-Sears and B. Downey with the statistical analyses is gratefully acknowledged. The L-Rubisco antiserum was a gift from N. Huner. This work was supported by a grant from CIDA to J. G. Gao and grant 36698 from the Natural Sciences and Engineering Research Council of Canada to A. Nassuth.

Accepted for publication 10 November 1992.

ABSTRACT

Gao, J. G., and Nassuth, A. 1993. Alteration of major cellular organelles in wheat leaf tissue infected with wheat streak mosaic rymovirus (Potyviridae). Phytopathology 83:206-213.

The alteration of cell organelles in wheat leaf cells systemically infected with wheat streak mosaic virus was quantitatively investigated at both light- and electron-microscopy levels. Nuclei significantly increased in size at an early stage of infection and contained dispersed heterochromatin. The nuclear envelope was frequently invaginated and had formed membrane-bound vesicles containing membranes, ribosomes, cylindrical inclusions, virus particles, and, occasionally, fibrils and mitochondria. Chloroplasts in infected tissue were smaller, frequently had extrusions, and contained far less starch than chloroplasts in healthy tissue. Many chloroplasts formed double membrane-bound invaginations in the envelope membrane. Virus particles and mitochondria were found within the invaginations. The viral infection also caused the chloroplast envelope's inner membrane to proliferate and fold repeatedly, dividing the stroma into numerous single membrane-bound fragments. Double membrane-bound elongated tubular structures accumulated in large quantities within the cytoplasm of infected cells. Labeling with rabbit antiribulose bisphosphate oxygenase-carboxylase serum proved that these structures were derived from chloroplasts, possibly via extrusions. The mitochondria in infected cells were lobed and contained degenerated cristae membranes. The peroxisomes became electron lucent and contained platelike inclusions. A large amount of electron-opaque material accumulated in the vacuole.

Additional keywords: cytological changes, plant:virus interaction, potyvirus, *Triticum aestivum*.

Wheat streak mosaic virus (WSMV) is a member of the rymovirus genus of the newly proposed Potyviridae (1,29), which causes streak mosaic symptoms on infected leaves of several cereals (2). Characteristic of all potyviruses is the induction of cytoplasmic cylindrical inclusions formed by a viral-encoded protein (CI); in addition, some potyviruses also induce nuclear inclusions formed by two other viral-encoded proteins (NIa and NIb) (6). Previous electron-microscopic observations showed that WSMV-infected cells contained cylindrical inclusions (visible in sections as pinwheels, scrolls, and laminated aggregates), nonviral crystals, virus aggregates, and fibrous masses in the cytoplasm but contained no inclusions in the nucleus of host cells (14,15,19,24,25). No consistent alteration of major cell organelles, other than a loss of grana thylakoids in chloroplasts, was noted (19). Our recent investigations of cereal leaf tissues by light microscopy revealed swollen nuclei and cytopathic structures within the nuclei of WSMV-infected cells (9). These cytopathic structures were distinct from the nuclear inclusions reported for other potyviruses (4,7,13) because they were less dense and did not stain well with protein stains (9). We also found that cellular contents, including chloroplasts, degraded more rapidly in WSMV-infected tissue than in control tissue (9). The relatively low resolution obtained with light microscopy did not permit further conclusions.

This paper reports on both light- and electron-microscopic observations of cell organelles during the course of WSMV infection of wheat leaf tissue. The results indicate that WSMV consistently

was able to induce conspicuous alterations of cellular organelles from 7 days postinoculation. Nuclei had increased in size, had altered heterochromatin profiles, and had invaginated envelope membranes. Chloroplasts were smaller, contained less starch, and had a proliferated inner envelope membrane and an invaginated envelope double membrane. Data concerning the number of organelles involved in each of these alterations and their apparent size were collected, to determine the extent of the virus-induced alterations.

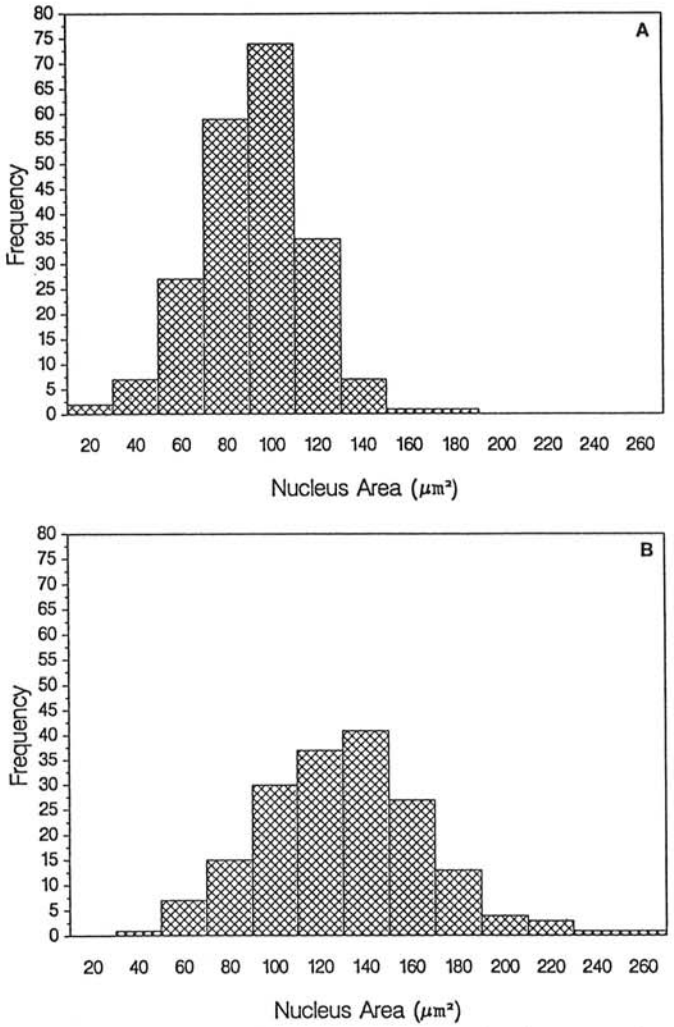

Fig. 1. Frequency distribution of apparent nuclear sizes, in square micrometers, measured in sections from **A,** healthy and **B,** infected second wheat-leaf mesophyll tissue (12 days postgermination). A total of 213 nuclei from healthy tissue and 180 nuclei from infected tissue were measured. These values pertain to cross-sectional areas of observed nuclei and not to absolute sizes.

MATERIALS AND METHODS

Plant material. Plants were grown and treated essentially as described previously (9). The first leaf of 5-day-old winter wheat (*Triticum aestivum* L.) cv. Fredrick seedlings was sap inoculated with a strain of WSMV (PV57; American Type Culture Collection, Rockville, MD). Symptoms, first visible in the second leaf 6–7 days postinoculation (dpi), appeared as light green dashes that turned yellow 8–9 dpi and expanded to fully developed streaks 10–12 dpi. Second leaves from healthy and mock-inoculated plants of similar age were used as uninfected controls.

Specimen preparation. Six to eight second leaves each from control and infected plants were collected 5, 6, 7, 9, 10, 11, and 12 dpi. The central segment (5-mm long) from each leaf was excised and fixed immediately at room temperature with 2.5% glutaraldehyde in 0.068 M sodium phosphate buffer, pH 6.8, for 4 h and was washed and postfixed with 2% OsO_4 in the same buffer for 3 h. The tissue was dehydrated in a graded ethanol series (30–100%), was transferred gradually to propylene oxide, and was infiltrated with Spurr's epoxy resin. The resin was polymerized at 60 C for 48 h.

Organelle size measurements. Sections, 1 μm thick, were cut with a Sorvall JB-4 microtome, were mounted on gelatin-coated glass slides, and were stained with 0.5% toluidine blue O in 0.1% sodium carbonate, pH 11.1. The stained sections were examined under a Zeiss-Jena Jenalumar contrast light microscope with Nomarski optics. Six micrographs, each covering 5,400 μm^2 and containing one to four nuclei and 20–70 chloroplasts, were taken from each sample with a Matic-Mot photomicrography system and were projected on a digitizer screen (GTCO Corp., Rockville, MD). The outline of each nucleus and chloroplast was traced, and the apparent sizes were subjected to statistical analysis.

Ultrastructural observations. Sections, 70- to 100-nm thick, were cut using an LKB Nova Ultratome (LKB, Upsala, Sweden) and were mounted on 4% collodion-dipped copper grids. Specimens were stained with 5% aqueous (w/v) uranyl acetate for 10 min, were rinsed in distilled water for 1 min, and were poststained with 2% (w/v) lead citrate for 5 min. A Jeol 100CX scanning transmission electron microscope (STEM; Jeol Ltd., Tokyo, Japan) was used at 80 kV in transmission mode to examine these specimens. The number of nuclei and chloroplasts showing various alterations was determined for each section and was compared by statistical analysis.

Immunogold labeling. Tissue was fixed in glutaraldehyde, was dehydrated in a graded ethanol series, and was embedded in LR white resin (9). Postfixation with osmium was omitted because it impaired the antibody binding. Sections, 100- to 150-nm thick, were cut using the LKB Nova Ultratome and were mounted on a slide precoated with 4% formvar. Sections were incubated with rabbit antiserum specific for the large subunit of ribulose bisphosphate carboxylase (obtained from N. Huner, University of Western Ontario, London, Canada) and with chicken antirabbit antibodies conjugated with 12 nm of colloidal gold particles (a gift from J. Greenwood, University of Guelph, Ontario) as described by Brown and Greenwood (3). Normal rabbit serum was used with

TABLE 1. Wheat streak mosaic virus-induced nuclear alterations[w]

Alterations	Treatments[x]				
	Healthy (7dpm)[y]	Healthy (11dpm)	Infected (7dpi)	Infected (9dpi)	Infected (11dpi)
Total number of nuclei examined	138	159	144	204	189
Nuclei with dispersed heterochromatin	5.6% b	0.4% b	36.6%	2.9% b	2.6% b
Nuclei with aggregated heterochromatin	2.4% b	5.3% ab	4.4% ab	7.3% ab	11.9% a
Nuclei with membrane invaginations	1.5% c	2.9% c	21.2% b	61.9% a	80.0% a
Mean number of invaginations per nucleus[z]	1.00 b	1.00 b	1.23 b	1.29 b	2.10 a

[w] Values followed by the same letter are not significantly different, with 95% confidence according to the Scheffé's test in a general linear model.
[x] The number of nuclei with a specific alteration is indicated as a percentage of the total number of nuclei examined.
[y] dpm = days post-mock-inoculation; dpi = days postinoculation.
[z] The mean number of invaginations per nucleus was calculated considering nuclei with invaginations only.

controls.

Statistical analyses. A completely randomized design was employed for all experiments. Each treatment contained six sections. Each section was obtained from the second leaf of six seedlings. Analysis of variance of the percentage of nuclei and chloroplasts showing alterations was performed using the SAS general linear model (SAS Institute, Cary, NC, version 6.06) on arcsin-transformed data. Range tests were performed using Scheffé's multiple ranges test at $\alpha = 0.05$. ANOVA also was performed on log-transformed data to obtain the size of nuclei and chloroplasts. Transformations were performed to normalize the data and to ameliorate heteroscedastic errors.

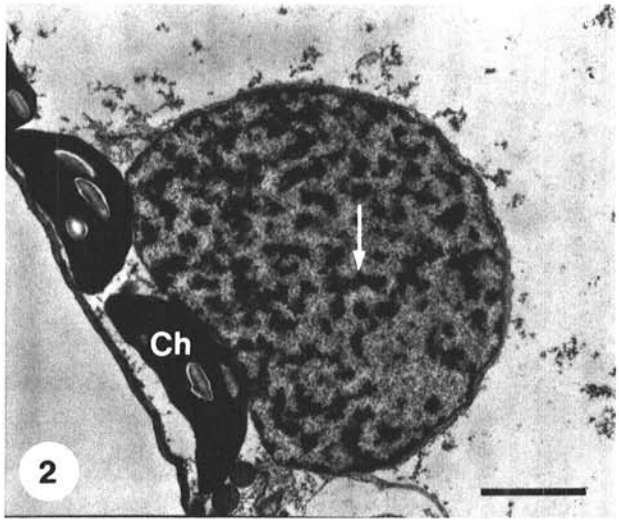

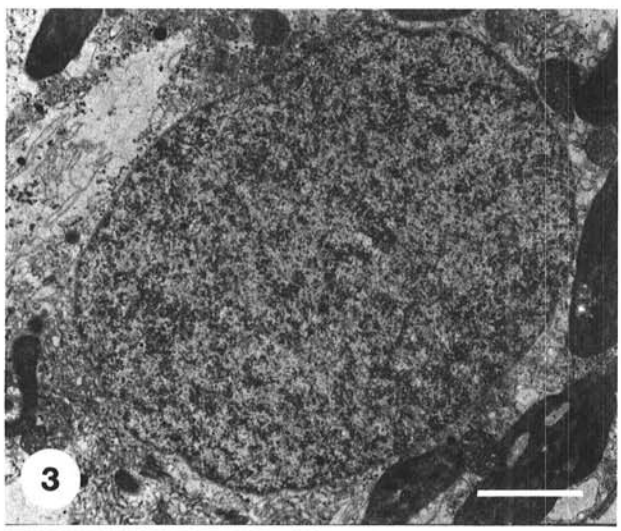

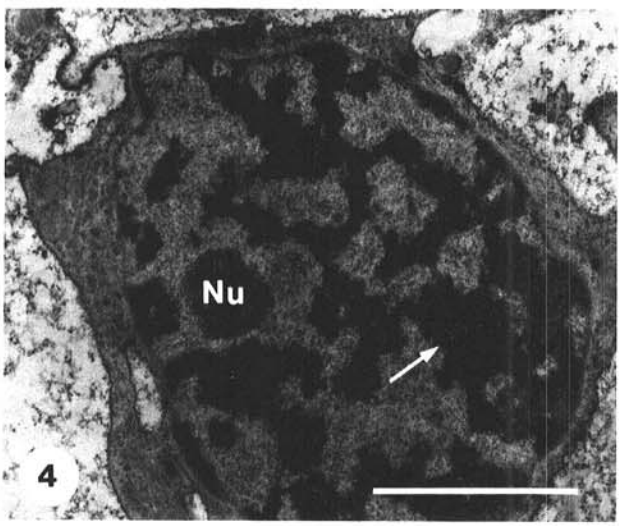

Figs. 2–4. Alteration of electron-dense nuclear heterochromatin (arrows) in WSMV-infected cells. **2,** nucleus in a healthy cell from the second leaf of a 12-day-old seedling. **3,** absence of electron-dense heterochromatin in the nucleus of a virus-infected cell from the second leaf of a 12-day-old seedling, 7 days postinoculation (dpi) of the first leaf. **4,** pyknotic nucleus of an infected cell, 11 dpi, with aggregated heterochromatin. Ch = chloroplast. Nu = nucleolus. Bars = 2.5 μm.

RESULTS

Alteration of the nucleus. An altered morphology of nuclei in WSMV-infected leaf tissue was observed at an early infection stage, 7 dpi, when compared to nuclei in healthy tissue. A significant increase in size was documented by measuring a total of 393 nuclei from healthy and infected tissue. Figure 1 shows that the main peak of frequency distribution shifted from 100 μm^2 in healthy cells (Fig. 1a) to 140 μm^2 in virus-infected cells (Fig. 1b). The frequency distribution was skewed slightly to the left in both cases, but a broader range of nuclear sizes was observed in infected cells. The backtransformed mean for healthy tissue was 90.31 μm^2, with a 95% confidence interval given by 82.89 μm^2 and 98.39 μm^2, versus 131.11 μm^2 for infected tissue, with a 95% confidence interval given by 120.34 μm^2 and 142.84 μm^2.

Electron-microscopic examination revealed not only an increase in size, but also a variety of ultrastructural alterations among the virus-infected cell nuclei (Table 1). The majority of the control nuclei had distinct and uniformly distributed heterochromatin throughout the period of investigation (10–17 days after germination; Fig. 2). However, the profile of the heterochromatin altered during the infection process. Dispersed heterochromatin was present in a large number of nuclei (36.6%) at 7 dpi (Fig. 3). Aggregated heterochromatin was found in only 4.4% of the nuclei at this time but gradually increased with infection to 11.9% of the nuclei at 11 dpi (Fig. 4; Table 1). Similar trends were seen in mock-inoculated tissue, but far fewer nuclei were involved (Table 1).

A second conspicuous ultrastructural change in cells of virus-infected leaf tissue was the invagination of the nuclear envelope membrane (Table 1). This process apparently formed double membrane-bound vesicles in the nuclei (Figs. 5–9). The number of nuclei with invaginations in infected tissue increased from 21.2%, 7 dpi, to 80%, 11 dpi. The invaginations initially were common along the edge of the nuclei and contained no visible internal structures (Fig. 5). Their size and number per nucleus increased as infection progressed, and membraneous structures and ribosomes were observed within them (Figs. 6 and 7; Table 1). At 11 dpi, the invaginations often contained membranes, ribosomes, virus particles, cylindrical inclusion bodies, and even mitochondria and a small vacuole (Fig. 8). Occasionally, fibrils also were found inside these nuclear membrane invaginations (Fig. 9). Far fewer nuclei in control tissue had invaginations and if so, had only one per nucleus (Fig. 2; Table 1).

Alteration of the chloroplasts. As shown in Figure 10, chloroplasts in WSMV-infected leaf cells were generally smaller than those in healthy cells, according to measurements of 2,919 chloroplasts in 12-day-old tissues (i.e., 7 days after mock or WSMV inoculation). The main peak of frequency distribution shifted from 8.5 μm^2 in healthy cells (Fig. 10a) to 7.0 μm^2 in infected cells (Fig. 10b). The backtransformed mean for healthy tissue was 9.31 μm^2, with a 95% confidence interval given by 8.57 μm^2 and 10.23 μm^2, versus 7.97 μm^2 for infected tissue, with a 95% confidence interval given by 7.49 μm^2 and 8.57 μm^2.

Ultrastructural observations also were made on 8,157 chloroplasts 9 days after mock (dpm) or WSMV inoculation (Table 2). A small percentage (0.8%) of the WSMV-infected chloroplasts were swollen and had an electron-lucent stroma (Fig. 11). Starch grains were absent from the majority of chloroplasts observed in sections of infected tissue (Figs. 11–16). Only 9% of the chloroplasts had starch exposed on the sections, compared to approximately 66% of the chloroplasts in sections of healthy leaf tissue (Table 2). Moreover, the starch grains that were present

in chloroplasts of virus-infected cells were considerably smaller than those present in chloroplasts of healthy cells (data not shown).

Chloroplast membranes, like nuclear membranes, were affected by the viral infection. Proliferated inner envelope membranes were observed in 6.1% of the chloroplasts in cells at 9 dpi (Table 2). These membranes folded repeatedly and divided the stroma into multiple layers, usually along the periphery of the chloroplasts (Fig. 12). Sometimes the compartmentation was localized and more complex (Fig. 13). Double membrane-bound vesicles of various sizes were found in 9.7% of the chloroplasts at this stage, especially at their tapered ends (Table 2, Fig. 14). A connection between such a vesicle and the cytoplasm was visible in some

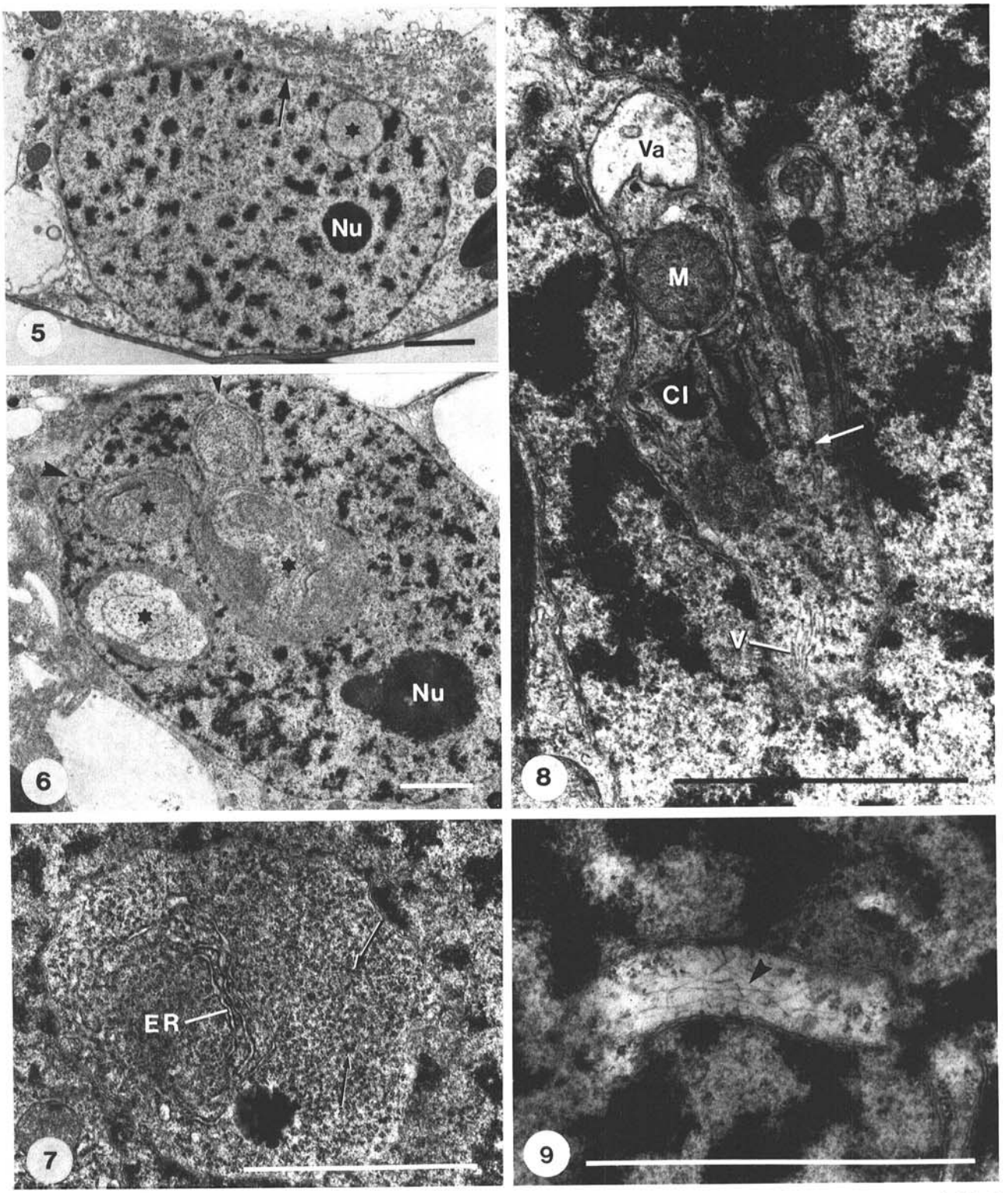

Figs. 5–9. Nuclear-membrane invagination induced by WSMV infection. **5,** a nucleus from a virus-infected cell at an early stage of infection, 7 days postinoculation (dpi), with an invaginated nuclear envelope (star). **6,** invaginations in contact with the cytoplasm (arrowheads) in the nucleus of a virus-infected cell, 11 dpi. **7,** a nuclear invagination containing cytoplasm enriched in an ER membrane (ER) and ribosomes (arrows), 11 dpi. **8,** a nuclear invagination containing ribosomes (arrow), cylindrical inclusions (CI), virus particles (V), a mitochondrion (M), and a small vacuole (Va), 11 dpi. **9,** a nuclear vesicle containing fibrils (arrowhead), 11 dpi. Nu = nucleolus. Bars = 2 μm.

sections (not shown), suggesting that at least part of the observed vesicles were invaginations. Virus particles were often present within these invaginations as well as, occasionally, mitochondria (Fig. 14). Formation of invaginations was not, unlike the stroma compartmentation, virus specific. A significantly lower percentage (2.7%) of chloroplasts in healthy cells had invaginations (Table 2).

Variable numbers of double membrane-bound elongated tubular structures were present in the cytoplasm of virus-infected cells (Fig. 12). These structures resembled the chloroplast extrusions that were observed most often at the tapered end (Fig. 15) and seemed to arise from the budding of these extrusions (Fig. 16). Antiserum raised against the large subunit of ribulose bisphosphate oxygenase-carboxylase (L-Rubisco) from rye reacted strongly with the contents of these cytoplasmic structures, confirming a chloroplastic origin (Fig. 17).

Alterations in the mitochondria, peroxisomes, and vacuoles. Compared to healthy cells (Fig. 18), in infected cells, mitochondria were lobed, had lost their internal membrane structure, and generally appeared electron lucent at 9 dpi (Fig. 19). Peroxisomes also became electron lucent following WSMV infection and frequently contained platelike inclusions (Fig. 19). Electron-opaque material was precipitated in the vacuolar lumen (Fig. 20).

DISCUSSION

The quantitative measurements in this paper document for the first time the significant impact of WSMV infection on the ultrastructure of cell organelles. The observation that many alterations occurred at a relatively early stage of infection (7–9 dpi) supports the hypothesis that at least some of these changes are related to an active response by the cell to the infection process and not to a virus-induced degradation process. We also observed a disruption of the organelles at later stages (from 11 dpi in this series of experiments; [9]) and assume that the formation of pyknotic nuclei represents the onset of nuclear degeneration.

Nuclei were affected most frequently. As early as 7 dpi, nuclei were larger, had dispersed heterochromatin, and often had an invaginated nuclear envelope membrane that apparently formed double membrane-bound invaginations (most likely the cytopathic structures previously observed by light microscopy [9]). The observation of mitochondria and vacuoles within these invaginations only at later stages suggests that they stay in contact with the cytosol for an extended period, if not indefinitely. The magnitude of these nuclear changes is quite high and seems to be characteristic for WSMV-infected cells. Some other viruses also induce diffuse heterochromatin (17,31) or nuclear invaginations (16,20, 21,28,30). However, the quantitative data have not been presented for these viruses, and therefore, the extent to which these changes have occurred is unclear. The published figures show relatively small nuclear invaginations that enclose only ground cytoplasm and, occasionally, membranes. A large-scale disappearance of electron-dense heterochromatin from nuclei has been reported only for tissue infected with pea enation mosaic virus (PEMV), and this coincided with, and was apparently related to, the replication of PEMV RNA (5,22,23) and the subsequent accumulation of viral particles in the nuclear lumen (26).

We did not observe the previously reported premature degradation of thylakoid membranes in chloroplasts of WSMV-infected cells (19) until 11 dpi or later. However, a significant number of chloroplasts showed other alterations, such as reduced size, reduction in the amount of stored starch, formation of divided stroma, and invaginations at earlier stages. We also found double membrane-bound sausage-shaped structures containing L-Rubisco in the cytoplasm of infected cells, which were most likely derived from budding chloroplast extrusions. A similar process has been proposed for tissue infected with pelargonium leaf curl virus (PLCV), a tombusvirus (18). This budding activity, together with the absence of starch grains, could be one reason for the significant reduction in chloroplast size.

No other potyvirus that induces a similar combination of chloroplast alterations has been found. Chloroplast extrusions but no tubular structures were observed in cells infected by bean yellow mosaic virus (BYMV) (31). An unexplained reduction in chloroplast size has been reported for mesophyll parenchyma cells infected with maize dwarf mosaic virus (MDMV) and sugarcane mosaic virus strain H (SCMV-H; [27]). Invaginations of the

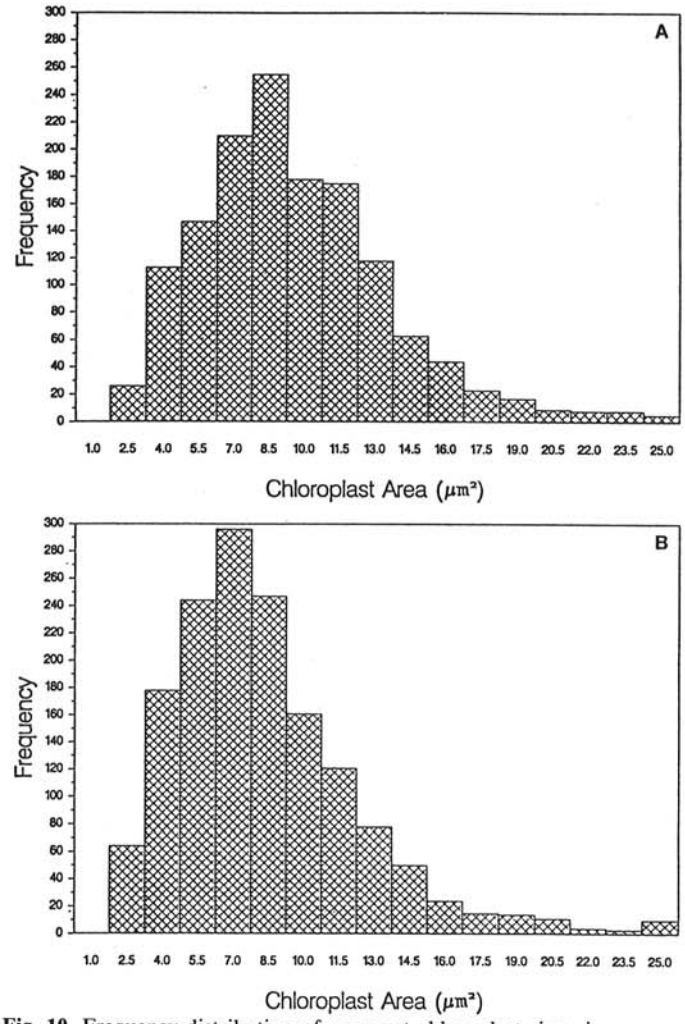

Fig. 10. Frequency distribution of apparent chloroplast sizes, in square micrometers, measured in sections from **A,** healthy and **B,** infected second wheat-leaf mesophyll tissue. A total of 1,399 chloroplasts from healthy tissue and 1,520 chloroplasts from infected tissue were measured. The obtained values pertain to cross-sectional areas of observed chloroplasts and not to absolute sizes.

TABLE 2. Wheat streak mosaic virus-induced chloroplast alterations[x]

Alterations	Treatments[y]	
	Healthy (9dpm)[z]	Infected (9dpi)
Total number of chloroplasts examined	4,061	4,096
Chloroplasts with starch grains	65.6% a	9.0% b
Chloroplasts with stroma compartmentation	0.0% a	6.1% b
Chlorplasts with extrusion	3.7% a	9.0% b
Chloroplasts with membrane invaginations	2.7% a	9.7% b
Swollen chloroplasts	0.0% a	0.8% b

[x] Values followed by the same letter are not significantly different, with 95% confidence according to the Scheffé's test in a general linear model.
[y] The number of chloroplasts with a specific alteration is indicated as a percentage of the total number of chloroplasts examined.
[z] dpm = days post-mock-inoculation; dpi = days postinoculation.

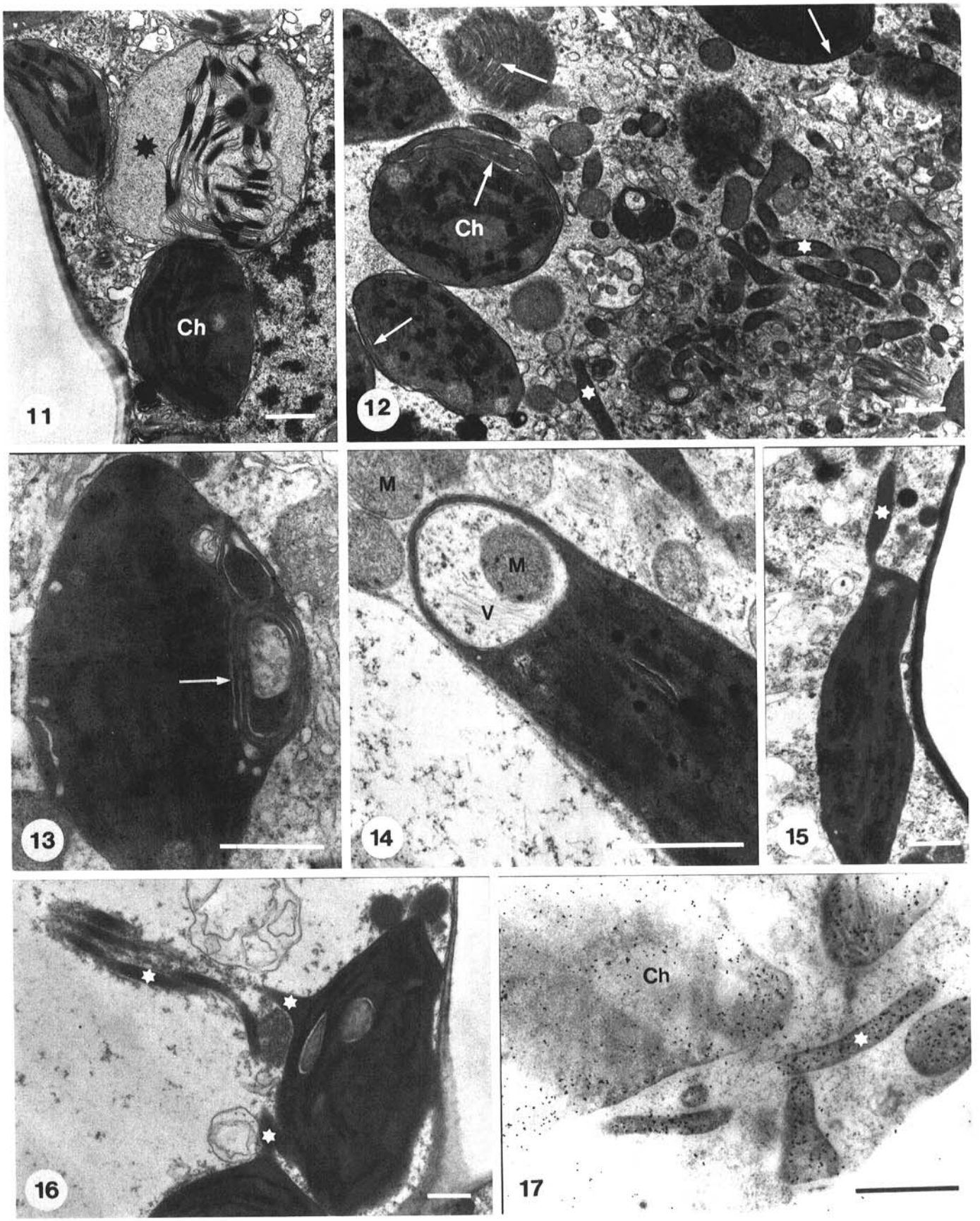

Figs. 11–16. Wheat streak mosaic virus-induced chloroplast alterations. **11,** swollen chloroplast with an electron-lucent stroma (star), 7 days postinoculation (dpi). The other two chloroplasts are representative of the majority of chloroplasts in infected cells. **12,** part of an infected cell containing double membrane-bound elongated tubular structures in the cytoplasm (star), 9 dpi. The chloroplasts have a proliferated inner membrane that fragments the stroma into multiple layers (arrows). **13,** chloroplast with a localized inner membrane proliferation (arrow), 11 dpi. **14,** chloroplast with a vesicle containing a mitochondrion (M) and viral particles (V), 11 dpi. **15,** chloroplast with extrusion (star), 9 dpi. **16,** budding of chloroplast extrusions (star), 7 dpi. **17,** immunolabeling with L-Rubisco antiserum, 9 dpi. Chloroplast and elongated tubular structures (star) in the cytoplasm are highly labeled, as indicated by the gold particles. Ch = chloroplast. Bars = 1 μm.

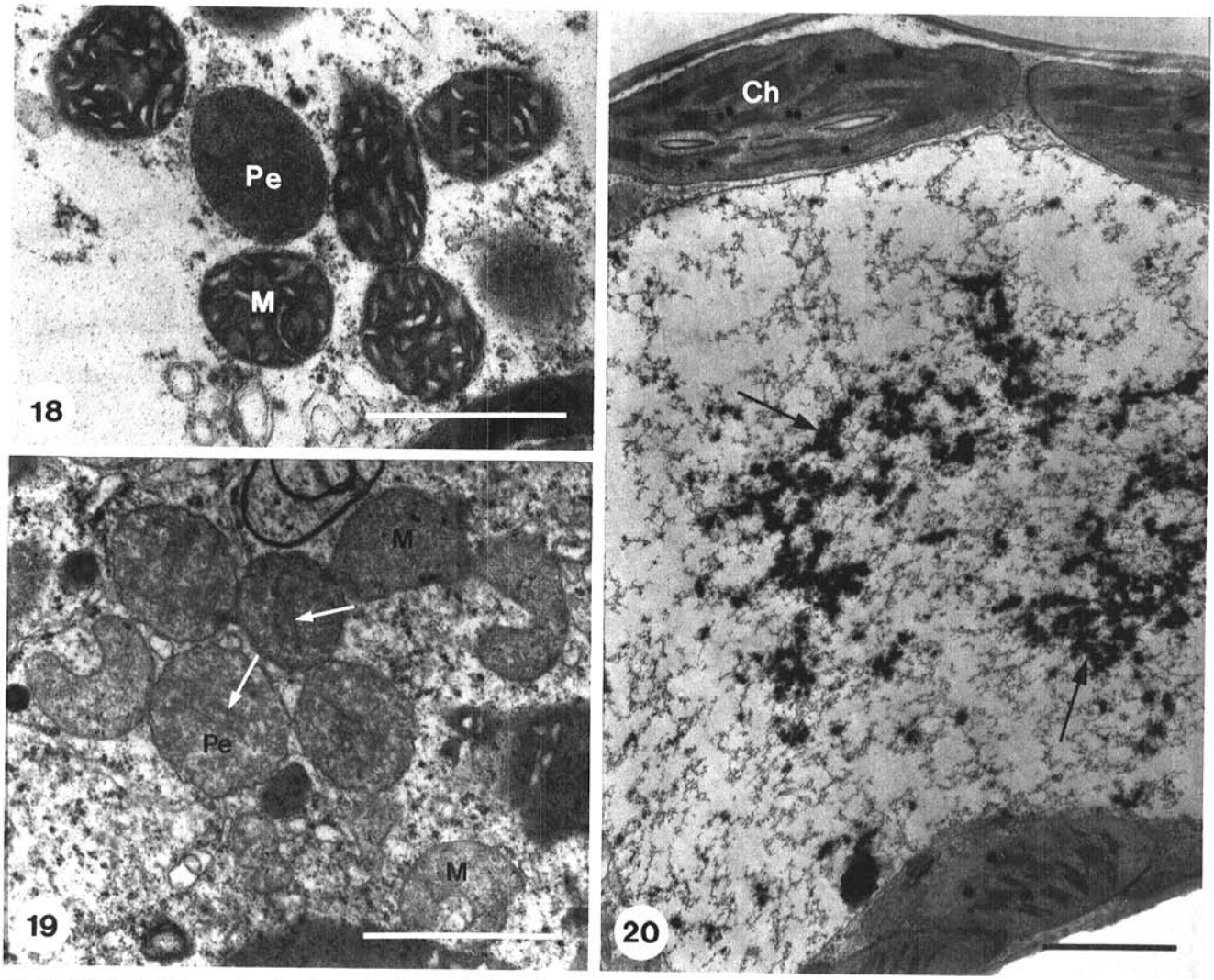

Figs. 18–20. Wheat streak mosaic virus-induced changes in the mitochondria (M), peroxisomes (Pe), and vacuoles. **18,** a group of mitochondria and a peroxisome in a healthy cell. **19,** a group of lobed mitochondria and peroxisomes from a virus-infected cell. There is a partial degradation of internal mitochondrial membranes, and there are platelike inclusions (arrows) in the peroxisomes. **20,** vacuolar lumen with electron-opaque material (arrows). Ch = chloroplast. Bars = 1 μm.

chloroplast envelope, containing mitochondria or endoplasmic reticulum, were also noted for pokeweed leaf cells infected with pokeweed mosaic virus (PMV) (12).

The fragmentation of chloroplast stroma was specific for WSMV-infected cells and requires proliferation of the inner envelope membrane. This process has not been reported for any other potyvirus-infected tissue, but it is a general phenomenon in tymovirus-infected cells (16). Tymoviruses also cause the formation of double membrane-bound vesicles in chloroplasts that have been implicated in a final viral-replication step (11,16). A similar role for the invaginations induced by WSMV is unlikely because they are larger, they are located mostly at the end of the chloroplasts, and they do not contain fibrillike material.

Our observations are consistent with the hypothesis that WSMV infection leads to an increase in cellular activity. The high number of nuclei containing dispersed heterochromatin at an earlier phase of infection (7 dpi) might indicate an enhanced rate of transcription. Also, membrane synthesis must have been enhanced to support the virus-induced proliferation of nuclear and chloroplast membranes. Whether these activities are related to a function of nuclei and chloroplasts in the viral-replication process remains to be seen. Virus-specific protein and putative RNA-replication intermediates were detected in chloroplast fractions of tissue infected with tobacco etch potyvirus and potato virus Y (8,10).

LITERATURE CITED

1. Barnett, O. W. 1991. *Potyviridae*, a proposed family of plant viruses. Arch. Virol. 118:139-141.
2. Brakke, M. K. 1971. Wheat streak mosaic virus. No. 48 in: Descriptions of Plant Viruses. Commonw. Mycol. Inst./Assoc. Appl. Biol., Kew, England.
3. Brown, M. J., and Greenwood, J. S. 1990. Involvement of the golgi apparatus in crystalloid protein deposition in *Ricinus communis* cv. Hale seeds. Can. J. Bot. 68:2353-2360.
4. Christie, R. G., and Edwardson, J. R. 1977. Light and electron microscopy of plant virus inclusions. Fla. Agric. Exp. Stn. Monogr. 9:55-88.
5. De Zoeten, G. A., Powell, C. A., Gaard, G., and German, T. L. 1976. *In situ* localization of pea enation mosaic virus infected plant tissue. Virology 70:459-469.
6. Dougherty, W. G., Carrington, J. C. 1988. Expression and function of potyvirus gene products. Ann. Rev. Phytopathol. 26:123-143.
7. Francki, R. I. B., Milne, R. G., and Hatta, T. 1985. Potyvirus group. Pages 183-217 in: Atlas of Plant Viruses. Vol. 2. CRC Pr., Inc., Boca Raton, FL.
8. Gadh, I. P. S., and Hari, V. 1986. Association of tobacco etch virus related RNA with chloroplasts in extracts of infected plants. Virology 150:304-307.
9. Gao, J. G., and Nassuth, A. 1991. Cytological changes induced by wheat streak mosaic virus in cereal leaf tissues. Can. J. Bot. 70:19-25.

10. Gunasinghe, U. B., and Berger, P. H. 1991. Association of potyvirus Y gene products with chloroplasts in tobacco. Mol. Plant-Microbe Interact. 4:452-457.
11. Hatta, T., and Matthews, R. E. F. 1976. Sites of coat protein accumulation in turnip yellow mosaic virus-infected cells. Virology 73:1-6.
12. Kim, K. S., and Fulton, J. P. 1969. Electron microscopy of pokeweed leaf cells infected with pokeweed mosaic virus. Virology 39:297-308.
13. Knuhtsen, H., Hiebert, E., and Purcifull, D. E. 1974. Partial purification and some properties of tobacco etch virus induced intranuclear inclusions. Virology 61:200-209.
14. Langenberg, W. G., and Schroeder, H. F. 1972. Disruptive influence of osmic acid and unbuffered chromic acid on inclusions of two plant viruses. J. Ultrastruct. Res. 40:513-526.
15. Lee, P. E. 1965. Electron microscopy of inclusions associated with wheat streak mosaic virus. J. Ultrastruct. Res. 13:359-366.
16. Lesemann, D. E. 1977. Virus group-specific and virus-specific cytological alterations induced by members of the tymovirus group. Phytopathol. Z. 90:313-336.
17. Martelli, G. P., and Russo, M. 1969. Nuclear changes in mesophyll cells of *Gomphrena globosa* L. associated with infection by beet mosaic virus. Virology 38:297-308.
18. Martelli, G. P., and Russo, M. 1972. Pelargonium leaf curl virus in host leaf tissues. J. Gen. Virol. 15:193-203.
19. McMullen, C. R., and Gardner, W. S. 1980. Cytoplasmic inclusion bodies induced by wheat streak mosaic virus. J. Ultrastruct. Res. 72:65-75.
20. Milne, R. G. 1966. Multiplication of tobacco mosaic virus in tobacco leaf palisade cells. Virology 28:79-89.
21. Paliwal, Y. C. 1970. Electron microscopy of bromegrass mosaic virus in infected leaves. J. Ultrastruct. Res. 30:491-502.
22. Powell, C. A., and De Zoeten, G. A. 1977. Replication of pea enation mosaic virus RNA in isolated pea nuclei. Proc. Natl. Acad. Sci. USA 74:2919-2922.
23. Powell, C. A., De Zoeten, G. A., and Gaard, G. 1977. The localization of pea enation mosaic virus-induced RNA-dependent RNA polymerase in infected peas. Virology 78:135-143.
24. Shepard, J. F. 1968. Occurrence of agropyron mosaic virus in Montana. Plant Dis. Rep. 52:138-141.
25. Shepard, J. F., and Carroll, T. W. 1967. Electron microscopy of wheat streak mosaic virus particles in infected plant cells. J. Ultrastruct. Res. 21:145-152.
26. Shikata, E., and Maramorosch, K. 1966. Electron microscopy of pea enation mosaic virus in plant cell nuclei. Virology 30:439-454.
27. Tu, J. C., Ford, R. E., and Krass, C. J. 1968. Comparisons of chloroplasts and photosynthetic rates of plants infected and not infected by maize dwarf mosaic virus. Phytopathology 58:285-288.
28. Van Der Scheer, C., and Groenewegen, J. 1971. Structure in cells of *Vigna unguiculata* infected with cowpea mosaic virus. Virology 46:493-497.
29. Ward, C. W., and Shukla, D. D. 1991. Taxonomy of potyviruses: Current problems and some solutions. Intervirology 32:269-296.
30. Weintraub, M., Agrawal, H. O., and Ragetli, H. W. 1973. Cytoplasmic and nuclear inclusions in leaf cells infected with *Datura* shoestring virus (DSV). Can. J. Bot. 51:855-861.
31. Weintraub, M., and Ragetli, H. W. J. 1966. Fine structure of inclusions and organelles in *Vicia Faba* infected with bean yellow mosaic virus. Virology 28:290-302.